Switchable Conductance in Functionalized Carbon Nanotubes *via* Reversible Sidewall Bond Cleavage

Elise Y. Li, Nicolas Poilvert, and Nicola Marzari*

Department of Chemistry and Department of Materials Science and Engineering, Massachusetts Institute of Technology, Cambridge, Massachusetts 02139, United States

ABSTRACT We propose several covalent functionalizations for carbon nanotubes that display switchable on/off conductance in metallic tubes. The switching action is achieved by reversible control of bond-cleavage chemistry in [1 + 2] cycloadditions *via* the $sp^3 \rightleftharpoons sp^2$ rehybridization that it induces; this leads to remarkable changes of conductance even at very low degrees of functionalization. Reversible bond-cleavage chemistry is achieved by identifying addends that provide optimal compensation between the bond-preserving through-space π orbital interactions with the tube against the bond-breaking strain energy of the cyclopropane moiety. Several strategies for real-time control, based on redox or hydrolysis reactions, *cis*–*trans* isomerization or excited-state proton transfer are proposed. Such designer functional groups would allow for the first time direct control of the electrical properties of metallic carbon nanotubes, with extensive applications in nanoscale devices.

KEYWORDS: first-principles calculations · functionalized carbon nanotubes · quantum conductance

Single-walled carbon nanotubes (SWNTs) have been investigated for manifold applications due to their special structural, mechanical, and electronic properties.[1] Chemical functionalizations of carbon nanotubes can add to their versatility, serving different purposes in chemical sensing, modifying the surface properties and solubilities, and facilitating the assembly, separation, and purification of CNTs.[2−4] Covalent chemical functionalizations[5,6] are especially relevant to manipulating the electronic properties of CNTs in nanoscale electric devices, such as molecular diodes or single molecular transistors.

In metallic CNTs, covalent functionalization of the sidewalls often reduces the electrical conductance by orders of magnitude due to the sp^3 hybridization brought upon by functionalization between CNT sidewall atoms and the addends which interrupts the π conjugation network of CNTs. This has been verified by first-principles calculations[7,8] as well as optical absorption spectra and electrical transport measurements.[9−12] In contrast, unlike the common [2 + 2] or [4 + 2] Diels–Alder reactions, where the sidewall bonds remain intact, in [1 + 2] cycloaddition functionalizations on armchair CNTs, first-principles calculations have shown that the strain of the cyclopropane ring introduced by divalent addends such as carbenes or nitrenes leads to sidewall bond cleavage, recovering sp^2 hybridization and thus preserving conductance.[8,13] It has already been observed that the formation of an ether-like oxygen bridge on the CNT sidewall in redox cycling gives high conductance due to sp^2 conjugation, in contrast to the low conductance observed in other functionalities,[14] and an early experimental confirmation of the effect of dichlorocarbene functionalization has just been found (N. Marzari and Q. Zhang, private communication).

In all of these studies, it appears that a molecular switch with the capability of controlling CNT conductance in response to an external optical, chemical, or electrical stimulus is highly desirable and could have applications for molecular devices, chemical sensors, and imaging. Recent theoretical studies have revealed the possibility of tuning bond-cleavage chemistry of [1 + 2] cycloadditions on CNTs through the orientation of the unsaturated π bonds of the addend with respect to the CNT surface.[15] In our previous study on the model system of dinitrocarbene-functionalized CNTs, we find that the bond-closed configuration is greatly stabilized when the plane of the addend π system bisects the base of the cyclopropane ring moiety. This stabilization effect was originally attributed to the enhanced interaction between the addend π and the cyclopropane Walsh orbitals, which weakens the antibonding interaction of the sidewall bond.[16] The bridgehead carbon atoms can reversibly rehybridize from sp^2 to sp^3 in response to addend π orientation, implying a switch-like behavior. Nevertheless, for

* Address correspondence to marzari@mit.edu.

Received for review December 14, 2010 and accepted May 18, 2011.

Published online May 18, 2011
10.1021/nn201022j

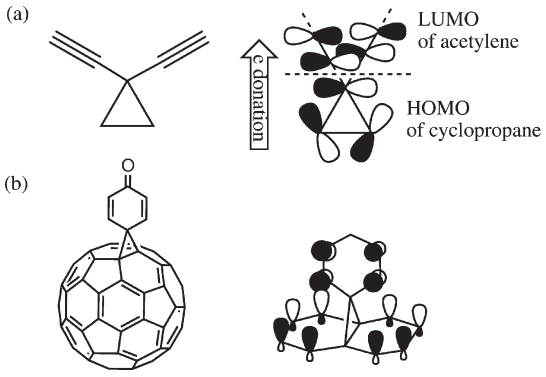

Scheme 1. Two possible contributing effects for closed CNT sidewall bond stabilization: (a) through-bond $\sigma-\pi$ interaction in cyclopropane and (b) through-space $\pi-\pi$ pericon-jugation in quinone-type methanofullerene.

dinitrocarbene-functionalized CNTs the bond-closed configuration is unstable. The addend prefers to rotate out of cyclopropane conjugation, resulting in only one stable open configuration that is impossible to manipulate. An isoelectronic carboxyl group was suggested to control bond cleavage by the intramolecular hydrogen bond,[15] but the hydrogen bond strength is too weak to offer bistability. Our calculations have shown that the closed-bond configuration is a saddle point rather than a local minimum.[17]

In this work, we systematically explore the cycloaddition functionalizations on carbon nanotubes using first-principles calculations. We characterize the structure and the electronic structure of armchair CNTs with various addends and provide an in-depth analysis of the underlying mechanisms that determine reversible bond-cleavage chemistry. We find that the high strain energy in the cyclopropane moiety can be compensated by a through-space π orbital interaction between the addend and the CNT which lowers the HOMO energy significantly in the closed-bond configurations. A bond opening or closing switch marked by large conductance change can therefore be devised by modulating the proximity between the addend π system and the tube surface with optical, chemical, or electrochemical means. We explore strategies for reversible bond cleavage using redox or hydrolysis reactions, *cis*−*trans* isomerization, or excited-state proton transfer and verify the marked change in CNT conductance with the addend in either the "on" or "off" configuration by quantum transport calculations.

RESULTS AND DISCUSSION

Mechanisms for Closed-Bond Stabilization. Previous studies[13,15] have shown that simple carbenes or nitrenes bearing only saturated moieties give an open sidewall bond, leaving very little room to maneuver for switching purposes. In this study, we will focus mostly on the interaction between unsaturated addends and the CNT surface and, more specifically, on the closed-bond stabilization offered by unsaturated addends in the perpendicular orientation. When considering only the cyclopropane moiety on the functionalized armchair carbon nanotubes, the simplest rationalization for closed-bond stabilization comes from the *through-bond $\sigma-\pi$ interaction*[16] (Scheme 1) which withdraws electron density from the HOMO of cyclopropane to the LUMO of acetylenes, causing a decrease in the bond length of the cyclopropane base but an increase for the lateral bond lengths. The bond variation in substituted cyclopropane, however, is typically smaller than 0.05 Å, suggesting this might be a less significant effect. On the other hand, a CNT is certainly a lot more complex than a cyclopropane. The sidewall bond-breaking chemistry of functionalized armchair carbon nanotubes is reminiscent of the valence tautomerism of 1,6-methano[10]annulene and the even more relevant methanofullerenes. During the search for improved electron-accepting organofullerens for photovoltaic applications, it was found that the quinone-type methanofullerenes or fluorenefullerenes that contain unsaturated moieties perpendicular to the surface of the fullerenes have a less negative first reduction potential than the parent C_{60} or other type of methanofullerenes by as much as 70 mV. The peak positions can be further tuned by electron-donating or electron-withdrawing groups attached to the addend. This phenomenon was ascribed to a *through-space $\pi-\pi$ interaction* which was called "periconjugation".[18−20] The intramolecular electronic interaction between the π orbitals of quinone and nearby carbon atoms of C_{60}, separated by a spiro carbon atom, results in more extended conjugation, which possibly improves its electron-accepting ability. As shown by the X-ray crystal structure, fullerene has an essentially [5]radialene-type electronic structure; that is, the [6,6] bonds possess more double bond character, while the [5,6] bonds are more single-bond-like. The fact that the isolated fluorenefullerenes were exclusively [6,6] fullerenes rather than [5,6]fulleroids also implies the existence of this stabilizing interaction. As a relevant digression here, it is worth mentioning that, unlike carbon nanotubes in which the sidewall bond lengths are largely affected by the addend identity, CNT curvature, and chirality, in organofullerenes, it is well-known that experimentally only the kinetic [5,6]-open and the thermodynamic [6,6]-closed adducts were observed in most cases, whereas [5,6]-closed and [6,6]-open counterparts are almost never found due to the unfavorable endocyclic pentagon double bond conjugation.[21] This might be the reason why dinitrocarbene substituent does not have the same rotational bond-cleavage effect in fullerenes as in CNTs.[15]

Unsaturated Addend Orientation Effect. In order to study the effect of addend π system orientation, we use 1,6-derivatized naphthalene (1,6-methano[10]annulene, **1**)

and pyrene (8,16-methano[2.2]metacyclophane-1, 9-diene, **2**) as molecular homologues of a functionalized CNT to investigate behaviors of different addends, following ref 13 (Scheme 2). The distance between the two bridgehead atoms 1 and 6 of **1**, d_{16}, is largely dictated by the substitutional group X.[22] The valence tautomerization between **1** (**2**) and bisnorcaradiene (cyclopropa[*e*]pyrene) corresponds to the open and closed configurations of a functionalized armchair CNT. A short d_{16} around 1.6 Å would correspond to a closed sidewall bond, and an elongated d_{16} over 2 Å would correspond to a broken sidewall C−C bond in a [1 + 2] cycloaddition-functionalized CNT. Prior to introducing more complicated effects such as the curvature of CNTs, we first study on these molecules the potential energy surface (PES) along d_{16} with different substitutional groups, in which the d_{16} is fixed at each point along the 1D-PES and all other degrees of freedom are fully relaxed unless further specified.

First of all, to rule out the orientation effect of unsaturated substitutional groups, we look at **2** with X = $C(CHO)_2$ (abbreviated as pyrene-$C(CHO)_2$ in the following) with the C═O double bonds pointing at different directions, as shown in Figure 1. As reported in previous studies, the addend prefers the unconstrained "flat" π plane as the most stable conformation in which the sidewall bond d_{16} is open, and in the constrained perpendicular π plane conformation, the d_{16} bond between two bridgehead atoms prefers closed. Between the two constrained perpendicular π plane conformations, however, we find that the closed bond configuration can be stabilized by about 0.2 eV more in the "O side" orientation in which the C═O double bonds lie closer to the pyrene backbone than in the "O top" orientation. This is a strong suggestion that the major closed-bond stabilization comes from periconjugation. The closed bond is stabilized the most when the addend π has maximal overlap with the pyrene backbone π system. On the other hand, the through-bond cyclopropane conjugation would not have been affected by the proximity between the oxygen atom and the pyrene surface.

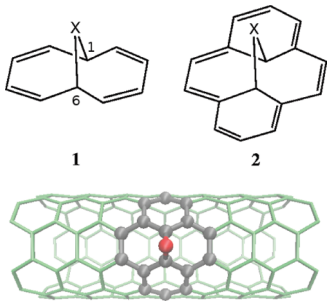

Scheme 2. Molecular homologues of a functionalized CNT: 1,6-derivatized naphthalene (1) and pyrene (2). The bond length between the bridgehead carbon atoms d_{16} depends primarily on the identity of the addend X. The similarity between the local structure of a [1 + 2] cycloaddition-functionalized CNT and the 2 is also shown.

Periconjugation Effect. The addend π bonds by nature prefer the flat orientation if they are left free to rotate, but they can be "locked" in place by a ring structure such as the cyclopentadienyl (C_5H_4) group. To further examine the strength of the periconjugation effect, we study the potential energy profile along d_{16} of **1** and **2** with various saturated and unsaturated ring substitutional groups as shown in Figure 2. Each point in Figure 2 corresponds to a full relaxation with only one geometry constraint, d_{16}, and the energy minimum under this constraint would correspond to the lowest energy ground state of the system, which was also confirmed by independent full relaxation calculations (without any constraints) and vibrational frequency calculations.

As can be seen clearly in Figure 2, for both **1** and **2**, the closed configuration is stabilized more when the

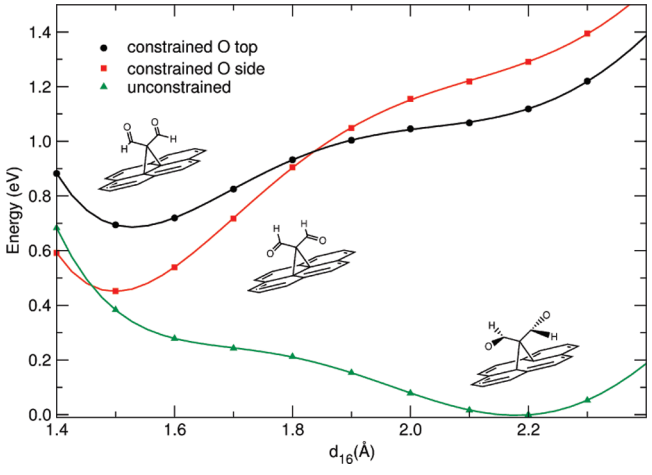

Figure 1. Potential energy surface as a function of d_{16} for 2 with X = $C(CHO)_2$ in different conformations. The closed-bond configuration is stabilized more when the C═O double bonds are closer to the pyrene backbone in the constrained perpendicular "O side" orientation.

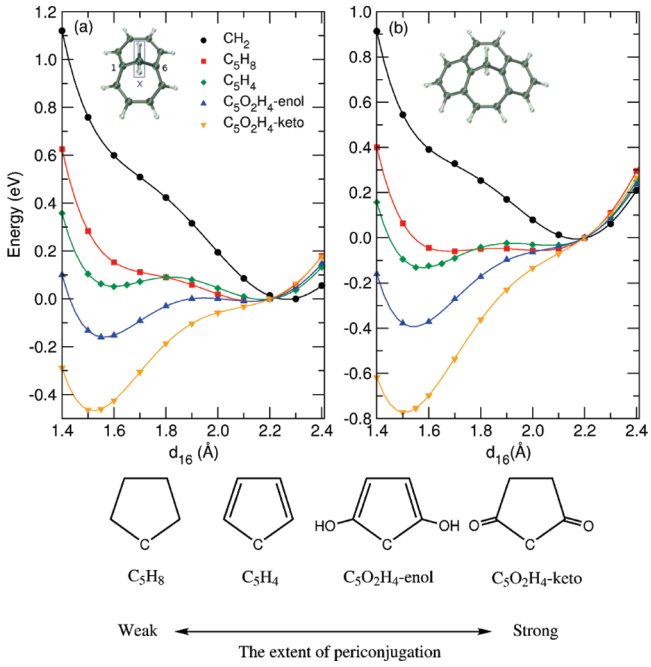

Figure 2. Potential energy surface as a function of d_{16} for (a) 1 and (b) 2 functionalized with ring substituents. The zeros are set at d_{16} = 2.20 Å to mark the release of roughly the same strain energy.

addend π system spans longer and leans toward the aromatic plane. The stabilization strength goes in the order of $C_5O_2H_4$-diketone > $C_5O_2H_4$-dienol > C_5H_4 diene, much greater than the saturated C_5H_8 or CH_2. For the case of **2**, the closed configuration is stabilized significantly more when X = $C_5O_2H_4$-diketone than when X = C_5H_4 by as much as 0.7 eV. This is another strong proof for the existence of the periconjugation effect as these substitutional groups are highly similar in structural motif and electronegativities. Any kind of inductive effect, if it exists, shall only differ slightly and shall not cause such a dramatic stabilization.

The origin of periconjugation stabilization can be revealed by an analysis of the eigenorbital evolution along d_{16}. The Walsh diagram of 1,6-methano[10] annulene (**1**) with X = CH_2 and X = $C_5O_2H_4$-keto is presented in Figure 3. The occupied a_2 and unoccupied b_1 are relatively unaffected by the d_{16} bond length and remain roughly flat. The two b_2 orbitals involve the antibonding interaction along d_{16} and are lowered in energy as the bond length increases. On the contrary, the two a_1 orbitals involve the bonding interaction and are raised in energy with increasing bond opening. The most striking difference between X = CH_2 and X = $C_5O_2H_4$-keto is the significant lowering in energy of b_2 in X = $C_5O_2H_4$-keto. The occupied b_2 orbital shows electron density delocalization between the π of naphthalene backbone and C═O double bonds and even switched ordering with a_2. This gives the overall stabilization of X = $C_5O_2H_4$-keto in closed configuration.

To this point, periconjugation is only expected to exist in perpendicular unsaturated addends. In our search among saturated addends, however, we find that, for both **1** and **2**, X = C_5H_8 is also more stabilized in the closed configuration than X = CH_2. This might be due to the relative rotational orientation of the C−H bonds adjacent to the spiro carbon atom with respect to the cyclopropane moiety. To verify this, we look at simpler substituents such as dimethylcarbene. We notice that the rotation of the methyl groups also introduces a slight periconjugation effect. The methyl groups can exist in two conformations, staggered or eclipsed with respect to the cyclopropane lateral bonds (Figure 4); both conformations predict an open sidewall bond with a shallow potential energy surface. The staggered methyl groups, as expected, give a more stable structure by 0.2 eV than the eclipsed one, but the energy barrier for the d_{16} bond to close in the eclipsed methyl conformation (0.12 eV) is only one-half of that of the staggered methyl conformation (0.19 eV). Figure 4 also shows the HOMO and HOMO−1 for both structures at d_{16} = 1.6 Å. The staggered molecule follows the same orbital ordering as in X = CH_2 and gives an a_2 HOMO and a b_2 HOMO−1, while in the eclipsed molecule, the two C−H σ bonds sticking toward the naphthalene backbone on both sides of the top C atom stabilize the b_2 orbital, showing a similar, although to a minor extent, through-space orbital interaction mechanism as in the case of perpendicular unsaturated substituents.

CNT Curvature Effect. The tautomerization between the bond-open and bond-closed form depends largely on the chirality and curvature of the CNT. In the case of

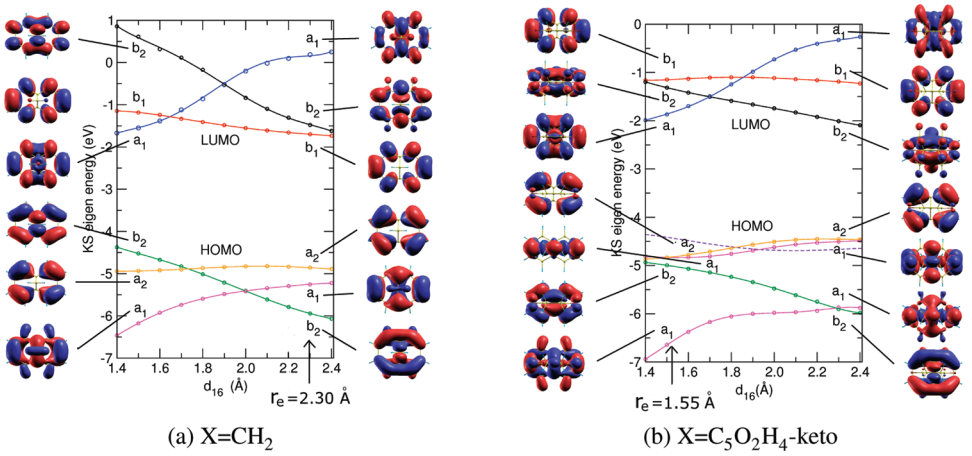

Figure 3. Walsh diagram along d_{16} of 1 for systems (a) without and (b) with periconjugation. The equilibrium bond lengths are also marked. The dashed curve in (b) is an orbital in the same energy window but with the density mostly located on the substituent and should be safely left out of discussion.

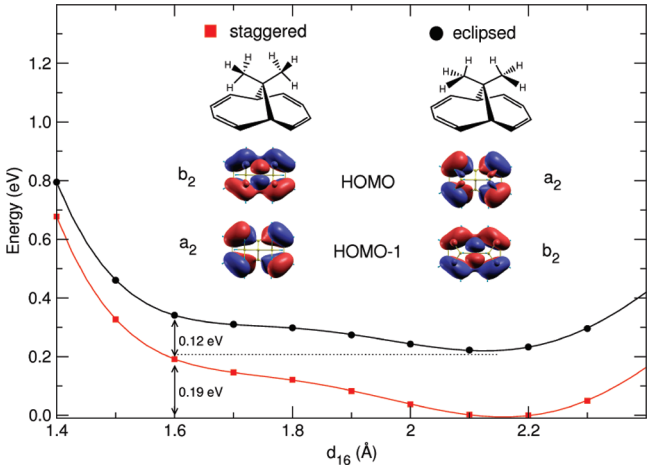

Figure 4. (a) Potential energy surface as a function of d_{16} for 1 with X = $C(CH_3)_2$ in staggered and eclipsed conformations. The frontier orbitals of two conformers at d_{16} = 1.6 Å are also shown here.

zigzag and armchair CNTs, two types of C−C bonds exist: the "axial" bonds A (the C−C bonds that are more "parallel" to the tube axis) and the "orthogonal" bonds O (the C−C bonds that lie more "perpendicular" to the tube axis). For both types of tubes, computational studies have shown that the A bond forms a closed-bond three-membered ring upon carbene cycloaddition and the O bond undergoes a sidewall bond opening upon carbene insertion.[12,23] The reaction energy defined as $\Delta E = E_{CNT-func} - E_{CNT} - E_{func}$ increases linearly as the curvature increases for both modes of addition reactions, but the functionalized CNT is always more stable in the open O bond configuation due to release of strain than the closed A bond configuration. Here we will focus our discussion only on armchair CNTs and on the [1 + 2] cycloaddition reactions to the orthogonal sidewall bond which opens up in most cases upon cycloaddition reaction, but may be brought back to the closed configuration in the presence of special closed-bond stabilizing effect. The orthogonal bonds in zigzag or chiral tubes should have similar behavior but will also depend specifically on the angle of each C−C bond with respect to tube axis.

As mentioned above, for the orthogonal bonds in armchair CNTs, the open-bond configuration is favored in high curvature CNTs so as to release the strain, but as the tube grows larger and the curvature decreases, the closed-bond configuration is gradually lowered in energy and eventually becomes more stable (for tubes larger than an (18,18)-CNT[13]). For small tubes, however, the competition between periconjugation and the curvature effect will determine the equilibrium between a closed and an open sidewall bond. We investigate a similar set of unsaturated substituents as in Figure 2 on a bent graphene model to represent the real CNT curvature effect. The carbon backbone of the 12 Å wide bent graphene nanoribbons is taken from CNTs with different curvatures, with the edge hydrogenated. The curvatures of the bent graphene nanoribbons are preserved by freezing the edge carbon atoms during later geometry optimizations.[24] Figure 5 shows the relaxed sidewall bond length of

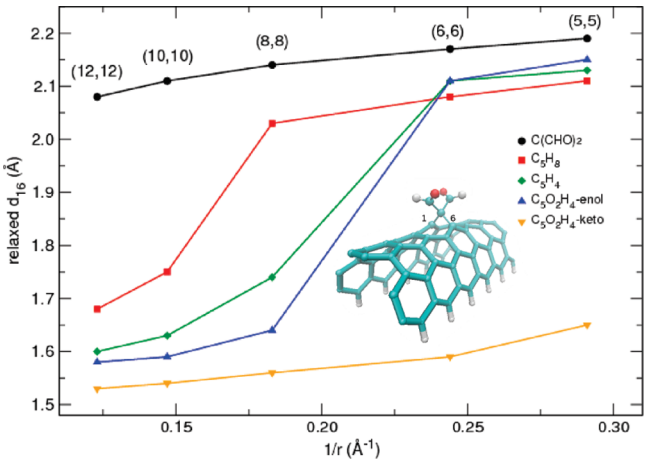

Figure 5. Sidewall equilibrium bond distance C_1-C_6 (d_{16}) for bent graphenes representing (*n*,*n*) CNTs. The edge carbon atoms (the hydrogenated ones) are fixed during structural relaxation to retain the curvature. All other atoms, including the addends, are fully relaxed without any constraints.

different bent graphene derivatives as a function of curvature. For unconstrained X = $C(CHO)_2$, the sidewall bond is always open up to the "(12,12)" bent graphene, while for X = $C_5O_2H_4$-keto that exhibits the strongest periconjugation effect, the sidewall bond is always closed even for the smallest (5,5) bent graphene.[25] Other addends showing intermediate periconjugation show transitions from open to closed at different critical curvatures.

Any single substituent among these on a carbon nanotube will not be useful for switching purposes since it will only give one configuration rather than a bistable ground state. Instead, the substituents studied in Figure 5 should be seen as basic molecular modules that can be chemically transformed between each other. For example, the cyclopentadienyl-functionalized (8,8) CNT, in principle, can be hydrogenated (if manipulated properly so that only the π bonds on the addend react) to give rise to the cyclopentane C_5H_8 substituent accompanied by a nanotube sidewall bond opening. Similarly, the cyclopentadiene ring can be cleaved to give some structure like X = $C(CHO)_2$, and a functionalized (10,10) or (12,12) tube shall respond with a conductance change. Indeed, two of the substituents in Figure 5, $C_5O_2H_4$-enol and $C_5O_2H_4$-keto, are already tautomers to each other and could perfectly serve as a switch for a (6,6) tube if one were able to stabilize selectively either enol or keto form in different chemical environments. Overall, the tubes with diameters around 0.8 to 1.4 nm have more flexible bond lengths and can be functionalized as conductance switches based on vertical transitions between different curves in Figure 5.

When a functionalized tube is switched from the open- to the closed-bond configuration, another complication that may arise is the relative stability between a closed axial bond A and a closed orthogonal bond O, and the possibility for the substitutional group to "migrate" to an adjacent C—C axial bond. For a carbene-functionalized (5,5) tube, the fully relaxed open O configuration is 1.2 eV more stable than the closed A configuration, but even the constrained closed O bond is still more stable than the closed A bond configuration by about 0.5 eV.[26] In the presence of periconjugation, the situation can be slightly more complicated since the distance between the addend π system and the tube surface will be different when the addend is attached to an A bond or an O bond. For a functionalized tube prepared as the "open" O bond (which is absolutely thermodynamically favored) than transformed to the "closed" O bond configuration chemically (to be discussed in the following section), we presume that as long as the chemical transformations on the addend part do not involve any biradicaloid mechanism, the addend is likely to remain on the same attachment site (*i.e.*, the O bond) and is unlikely to "walk" to an adjacent A bond. In any case, for conduction switching purposes, both a closed O and a closed A bond will give low conductivities since they both disrupt severely the π manifold of the CNT.

Conduction Switching on Functionalized Carbon Nanotubes. Apart from the keto—enol tautomerization mentioned in the last section, here we propose several other switching mechanisms that could suit different experimental conditions and device setups. These switches can be controlled by chemical reactions or optical excitations. Figure 6 gives an overview for the switching mechanisms we propose. The switching can be achieved by breaking a bond in the five-membered ring, for example, in a hydrolysis reaction of an ester or an amide bond (Figure 6a), or by removal of the C=O double bonds, for example, by reducing the diketone to a diol (Figure 6b). Alternatively, the switching can also take place by tuning the spatial proximity between the addend π system and the tube surface, for example, by imine *cis*—*trans* isomerization (Figure 6c), or by

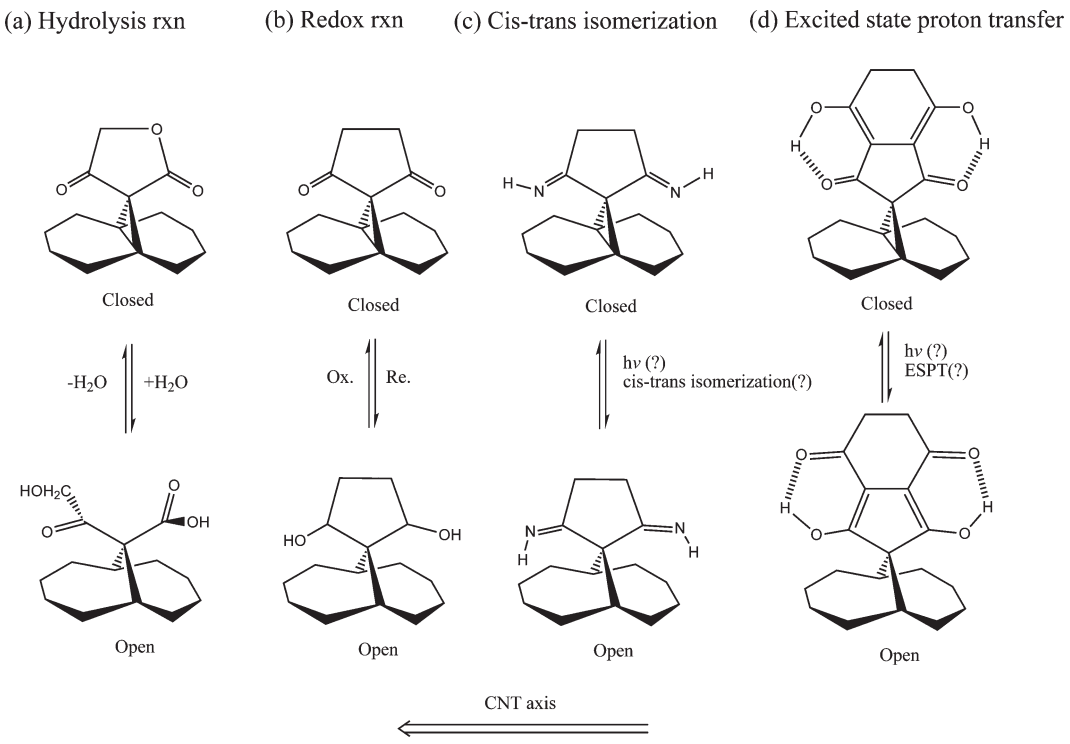

Figure 6. Proposed conductance switching mechanism in functionalized armchair CNTs. The addends are attached to the C−C bonds perpendicular to the CNT axis labeled on the bottom of the figure.

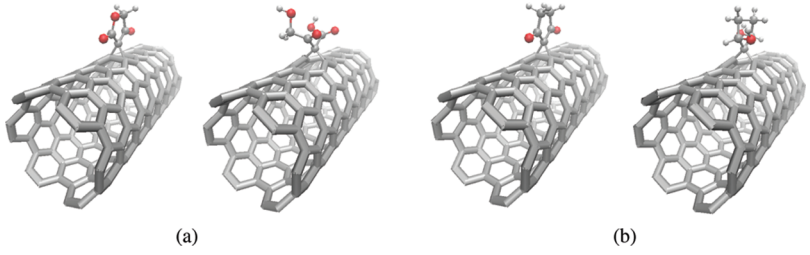

Figure 7. Relaxed structures of a functionalized (6,6) CNT with (a) lactone and free carboxyl groups shown in Figure 6a and (b) diketone and diol addends shown in Figure 6b. The CNT sidewall bond is closed with the lactone or diketone substituent and is open with free carboxyl groups or diol addends.

shifting the conjugation on the addend (keto−enol transformation) in excited-state proton transfer (ESPT) (Figure 6d). For all the systems considered in the following, we consider the addition reaction to the orthogonal sidewall bond of the armchair (6,6) CNT and perform in each case full structural relaxations in a supercell containing five primitive unit cells (*i.e.*, 120 CNT carbon atoms).

Switching *via* Chemical Reactions. As shown in Figure 7, hydrolysis and redox reaction products successfully give stable open and closed configurations, as expected. The CNT sidewall bond is closed with the lactone or diketone substituent and is open with free carboxyl groups or diol addends. On the basis of our study of the curvature effect using the bent graphene model (Figure 5), we predict that the hydrolysis switch should be able to work for tubes ranging from (6,6) to (12,12), and the redox switch should work for tubes from (6,6) to at least (8,8) or even (10,10). From a synthetic point of view, attaching such functional groups to a CNT sidewall should not be feasible. For example, to prepare a hydrolysis switch, a malonate moiety can be introduced relatively easily by the well-estabilizhed Bingel reaction.[9,27] Experimentally, the reaction process in a solution possibly will require extra care to avoid unwanted damage to the tube surface under redox or acid/base conditions.

Switching *via* Optical Excitations. An optically controlled switch, in contrast, is less straightforward to design since the bond breaking or conjugation shifting in response to optical stimulation is more demanding on the overall molecular electronic structure. We propose tentatively the imine *cis*−*trans* isomerization and the excited-state proton transfer (ESPT) as optically controlled conductance switches. In the imine *cis*−*trans* isomerization, the open-closed sidewall bond

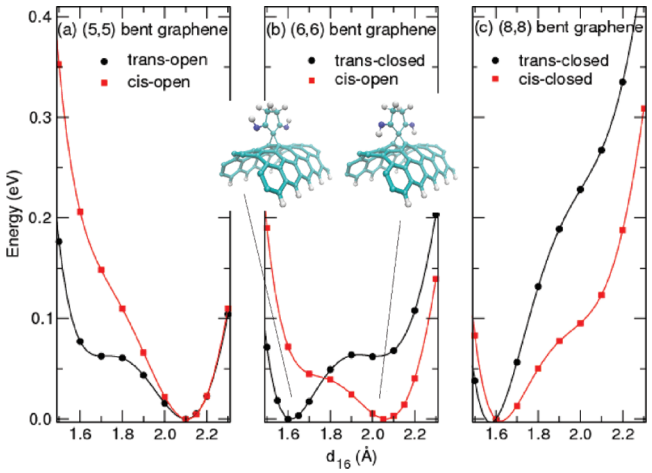

Figure 8. Potential energy surface as a function of d_{16} for (5,5), (6,6), or (8,8) bent graphenes functionalized with X = *cis*- or *trans*-cyclopentadiimine. The relaxed structure of functionalized (6,6) bent graphene in the equilibrium bond length is also shown.

transformation is determined by the conformation of the N—H bond. This is achieved due to the fact that the strength of periconjugation is highly sensitive to the spatial proximity between the addend double bonds and the tube surface. It is known that in the fullerene counterpart, when two benzene rings are fused to the quinone moiety in the quinone-type methanofullerenes, the first reduction potential becomes more negative rather than more positive; that is, it becomes an even worse electron acceptor. This was accounted for by the steric hindrance effect between the "peri" hydrogens and the surface of C_{60}.[20] We study the ground-state potential energy surface of bent graphenes with X = *cis* or *trans* cyclic imines (we arbitrarily differentiate the two conformers as *cis* (when the peri-hydrogens point toward the tube surface) or *trans* (when the peri-hydrogens point away from the tube surface) isomers; see Figure 8) and found that at a critical curvature (in this case the bent graphene representing (6,6) CNT) a change as simple as a *cis*—*trans* isomerization would indeed induce a sidewall bond cleavage, while tubes smaller or larger than this critical size will have only closed or only open configurations for both isomers. In practice, however, the imine *cis*—*trans* isomerization will be difficult, if not impossible, to manage. Unlike the well-known light-initiated *cis*—*trans* isomerization of azobenzenes or stilbenes, photoinduced rotation along the C═N (or C═C and N═N) double bonds for simple imines (or ethylene and diimide) so far has not been observed experimentally due to technical difficulties (the excitation energy needs to be extremely high; around 100—200 nm far-UV light). However, numerous theoretical investigations have proven that photoisomerization is likely to happen through a conical intersection between the ground and the first excited state at the femtosecond time scale.[28—30]

For ESPT (shown in Figure 6d), we are able to locate two local minima for the normal (the cyclopentadiketone) and the proton-transferred tautomer (the cyclopentadiene diol) for the hydrogenated substituents alone (not attached to the CNT). The forward and reverse reaction barriers in the ground state for this proton transfer reaction are 0.50 and 0.28 eV, respectively. Nevertheless, when these addends are attached to the CNT, both normal and tautomer substituents give an open sidewall bond for a (6,6) tube and both give a closed sidewall bond for a (7,7) tube. This again demonstrates the "spatial sensitivity" of periconjugation. When the C═O double bonds of the cyclopentadione are attracted toward the hydroxyl groups, the distance between the C═O double bonds and CNT surface increases slightly, the periconjugation decreases, and the sidewall bond opens.

Switching *via* Quinone—Quinol Transformation. Alternatively, an intramolecular hydrogen bond can be tuned to control the distance between the C═O double bond and the tube surface. As shown in Figure 9, the hydrogen-bonded cyclopentadione and the quinol moiety shall render the sidewall bond of a (6,6) tube open, but the intramolecular hydrogen bonding can be easily removed by either an oxidation or an acid/base reaction. The diketone C═O double bonds are therefore released, and the (6,6) CNT sidewall bond will be closed. The oxidation of a quinol into a quinone can happens in a milder condition than the diol oxidation, which should be less harmful to the CNT itself and more favorable in this respect.

Quantum Conductance of Functionalized CNTs. The conductivity of the proposed switches in the on and off states on CNTs is also investigated. Figure 10 shows the quantum conductance of a singly functionalized (6,6) carbon nanotube with either lactone/acid or the diketone/diol addend pairs designed in

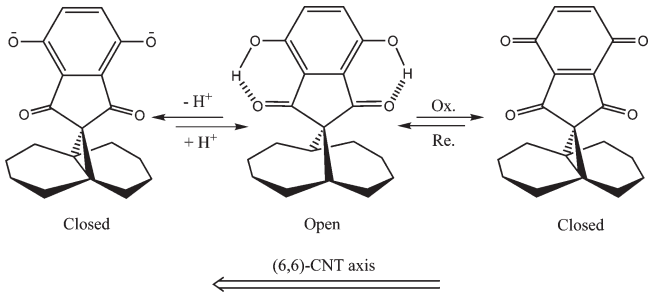

Figure 9. Proposed conductance switching mechanism by tuning the intramolecular hydrogen bonding between the quinol and the cyclopentadione moiety. On a (6,6) CNT, the hydrogen-bonded addend (in the middle) shall render the CNT sidewall bond open, while removal of the hydrogen bonds will induce a bond closure.

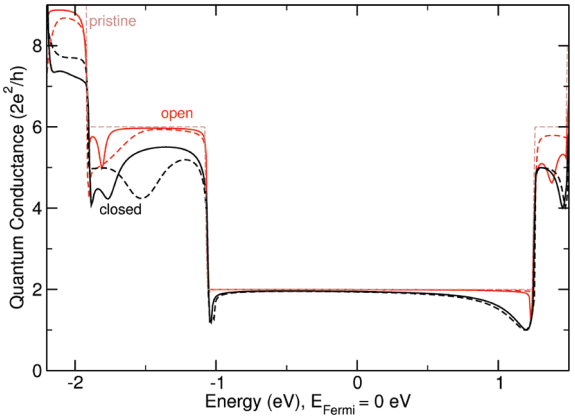

Figure 10. Quantum conductance of an infinitely long (6,6) carbon nanotube with a single functionalization. The solid lines correspond to the lactone/acid addend pair, and the dashed lines correspond to the diketone/diol addend pair. The red color is for the open (acid and diol), and the black color is for the closed (lactone and diketone) conformations. The quantum conductance of the pristine tube is also given by the brown dashed line as a reference. The quantum conductance depends more on the open or closed conformations rather than on the specific addend identity in a wide energy range around the Fermi energy.

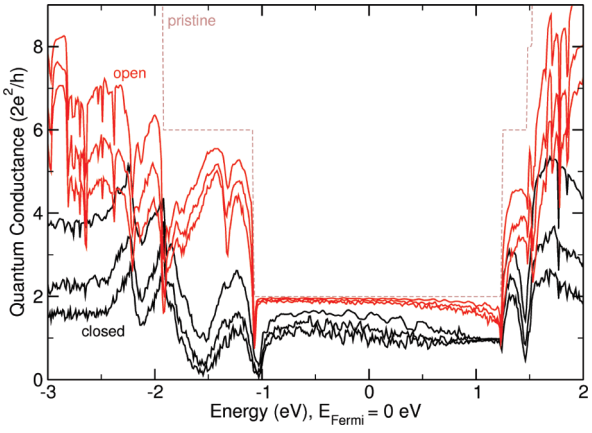

Figure 11. Average quantum conductance (in units of $2e^2/h$) of 20 randomly functionalized (6,6) carbon nanotubes with 10, 20, or 30 addends. Both types of addends are considered (ketone in black and diol in red). Inside a given set of conductance curves (black or red), the highest curve represents 10 addends, and the lowest curve represents 30 addends. The quantum conductance of a pristine (6,6) carbon nanotube is given as a dashed line as a reference.

Figure 6a,b. While the conductances for the open configurations (the acid and the diol) are negligibly affected and can hardly be distinguished from the pristine conductance around the Fermi level, the conductances of the closed configurations (the lactone and the diketone) are lower. Nevertheless, the conductances at the Fermi level for both cases remain close.

The difference, however, is greatly magnified in multiple functionalized CNTs. Figure 11 shows the

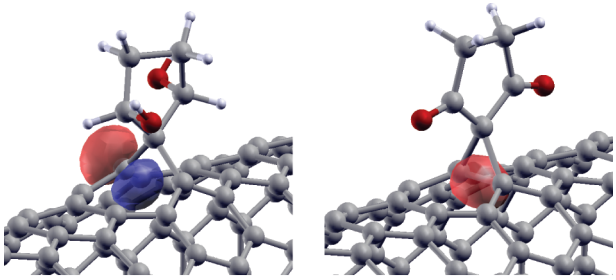

Figure 12. Visualization of (a) one of the two "p_z"-like Wannier orbitals in the open conformation and (b) the "σ"-like orbital in the closed conformation in the diketone/diol addend pair. The strong scattering introduced in the closed conformation is due to the disappearance of the two p_z Wannier orbitals which disrupts the π manifold of the CNT.

quantum conductance of a 22, 47, or 67 nm long (6,6) CNT functionalized with 10, 20, or 30 addends, respectively, for the diketone/diol switch pair. The strong scattering of the π electrons in a window of about 2 eV around the Fermi energy in the closed conformation is evidenced by the increasing drop in quantum conductance with the degree of functionalization. The quantum conductance is reduced by about 13% from 1 to 10 addends, another 23% from 10 to 20, and at last another 29% from 20 to 30 addends in the closed (diketone) case. On the contrary, the open (diol) case shows only a 2% reduction from 1 to 10 addends, another 3% from 10 to 20, and another 3% from 20 to 30 addends. The average quantum conductance at the Fermi level functionalized with 30 addends in closed conformation drops to about 0.87, whereas it remains at about 1.84 in the open case. The fundamental origin of this strikingly different behavior goes back to the earliest prediction: the sidewall bond breakage in the open configuration preserves the π network, while in the closed conformation, only a σ-like Wannier function is left, destroying locally the π conjugation, as shown in Figure 12.

CONCLUSION

In conclusion, we have identified the role of through-space periconjugation in controlling the sidewall bond-cleavage chemistry in [1 + 2] cycloaddition-functionalized CNTs. We have predicted that a functional group similar to the $C_5O_2H_4$-ketone moiety with carefully arranged π orientations with respect to the CNTs could strongly stabilize the closed conformation even for CNTs with the curvature as high as that of a (6,6) tube. We have proposed possible conduction switching mechanisms that cover different CNT diameters and can be applied in different experimental environments and device setups, controlled by chemical, electrochemical, or optical means. Our transport calculation verifies that the quantum conductance changes significantly in the on or off state. These switches, if realized experimentally, should have practical applications in nanoscale electrical devices and sensing.

METHODS

Computational Details. All calculations are performed using density functional theory in the Perdew–Burke–Ernzerhof generalized-gradient approximation (PBE-GGA)[31] with plane wave basis sets, periodic boundary conditions, and Vanderbilt ultrasoft pseudopotentials[32] as implemented in the Quantum-ESPRESSO package.[33] Next, 30 and 240 Ry cutoffs or higher are chosen for the wave functions and the charge density, respectively. For isolated molecular systems, a large supercell is constructed so that the distance between periodic images is at least 8 Å to ensure negligible interactions. The nudged elastic band (NEB)[34] method was used for obtaining transition-state geometries and reaction paths. For the carbon nanotube calculations, our supercell includes five unit layers of carbon atoms for a given (*n*,*n*) CNT plus the functional group. A 1 × 1 × 4 *k*-point sampling is used for structural optimization with a cold smearing of 0.03 Ry.[35] All components of all forces are converged to within 10^{-3} Ry/bohr, corresponding to less than 0.026 eV/Å in a relaxation calculation. The quantum conductance at zero bias is calculated using the Landauer formalism[36] in a basis of maximally localized Wannier functions (MLWF)[7] as implemented in the Wannier90[37] code.

Acknowledgment. The authors thank Y.-S. Lee, T. Swager, and J. Schnorr for helpful suggestions and discussions. This work was supported by the Chesonis Family Foundation and MIT's Institute for Soldier Nanotechnologies of the U.S. Army Research Office (ISN-ARO) under award number W911NF–07D–0004).

Supporting Information Available: More computational details on the bent graphene model and quantum conductance calculations. This material is available free of charge *via* the Internet at http://pubs.acs.org.

REFERENCES AND NOTES

1. de Heer, W. A. Nanotubes and the Pursuit of Applications. *MRS Bull.* **2004**, *29*, 281–285.
2. Burghard, M.; Balasubramanian, K. Functionalization of Carbon Nanotubes. *Small* **2005**, *1*, 180–192.
3. Tasis, D.; Tagmatarchis, N.; Bianco, A.; Prato, M. Chemistry of Carbon Nanotubes. *Chem. Rev.* **2006**, *106*, 1105–1136.

4. Prato, M. Controlled Nanotube Reactions. *Nature* **2010**, *465*, 172–173.
5. Sun, Y.-P.; Fu, K.; Lin, Y.; Huang, W. Functionalized Carbon Nanotubes: Properties and Applications. *Acc. Chem. Res.* **2002**, *35*, 1096–1104.
6. Dyke, C. A.; Tour, J. M. Covalent Functionalization of Single-Walled Carbon Nanotube for Materials Applications. *J. Phys. Chem. A* **2004**, *108*, 11151–11159.
7. Lee, Y.-S.; Marzari, N. Band Structure and Quantum Conductance of Nanostructures from Maximally Localized Wannier Functions: The Case of Functionalized Carbon Nanotubes. *Phys. Rev. Lett.* **2005**, *95*, 076804.
8. Lopez-Bezanilla, A.; S. Latil, F. T.; Blase, X.; Roche, S. Effect of the Chemical Functionalization on Charge Transport in Carbon Nanotubes at the Mesoscopic Scale. *Nano Lett.* **2009**, *9*, 940–944.
9. Kamaras, K.; Itkis, M. E.; Hu, H.; Zhao, B.; Haddon, R. C. Covalent Bond Formation to a Carbon Nanotube Metal. *Science* **2003**, *301*, 1501.
10. Strano, M. S.; Dyke, C. A.; Usrey, M. L.; Barone, P. W.; Allen, M. J.; Shan, H.; Kittrell, C.; Hauge, R. H.; Tour, J. M.; Smalley, R. E. Electronic Structure Control of Single-Walled Carbon Nanotube Functionalization. *Science* **2003**, *301*, 1519–1522.
11. Klinke, C.; Hannon, J. B.; Afzali, A.; Avouris, P. Field-Effect Transistors Assembled from Functionalized Carbon Nanotubes. *Nano Lett.* **2006**, *6*, 906–910.
12. Kanungo, M.; Lu, H.; Malliaras, G. G.; Blanchet, G. B. Suppression of Metallic Conductivity of Single-Walled Carbon Nanotubes by Cycloaddition Reactions. *Science* **2009**, *323*, 234–237.
13. Lee, Y.-S.; Marzari, N. Cycloaddition Functionalizations To Preserve or Control the Conductance of Carbon Nanotubes. *Phys. Rev. Lett.* **2006**, *97*, 116801.
14. Goldsmith, B. R.; Coroneus, J. G.; Khalap, V. R.; Kane, A. A.; Weiss, G. A.; Collins, P. G. Conductance-Controlled Point Functionalization of Single-Walled Carbon Nanotubes. *Science* **2007**, *315*, 77–81.
15. Lee, Y.-S.; Marzari, N. Cycloadditions To Control Bond Breaking in Naphthalenes, Fullerenes, and Carbon Nanoutbes: A First-Principles Study. *J. Phys. Chem. C* **2008**, *112*, 4480–4485.
16. Scott, L. T.; Cooney, M. J.; Otte, C.; Puls, C.; Haumann, T.; Boese, R.; Carroll, P. J.; Smith, A. B.; de Meijere, A. Enhancement of Through-Space and Through-Bond p-Orbital Interactions—Syntheses and Properties of Permethylated and Perspirocyclopropanated Cyclotetradeca-1,3,6,9,12-pentayne. *J. Am. Chem. Soc.* **1994**, *116*, 10275–10283.
17. Our calculations have shown that the closed-bond configuration is a saddle point rather than a local minimum.
18. Eiermann, M.; Haddon, R. C.; Knight, B.; Li, Q. C.; Maggini, M.; Martin, N.; Ohno, T.; Prato, M.; Suzuki, T.; Wudl, F. Electrochemical Evidence for Through-Space Orbital Interactions in Spiromethanofullerenes. *Angew. Chem., Int. Ed. Engl.* **1995**, *34*, 1591–1594.
19. Keshavarz-K, M.; Knight, B.; Haddon, R. C.; Wudl, F. Linear Free Energy Relation of Methanofullerene C61-Substituents with Cyclic Voltammetry: Strong Electron Withdrawal Anomaly. *Tetrahedron* **1996**, *52*, 5149–5159.
20. Knight, B.; Martin, N.; Ohno, T.; Orti, E.; Rovira, C.; Veciana, J.; Vidal-Gancedo, J.; Viruela, P.; Viruela, R.; Wudl, F. Synthesis and Electrochemistry of Electronegative Spiroannelated Methanofullerenes: Theoretical Underpinning of the Electronic Effect of Addends and a Redutive Cyclopropane Ring-Opening Reaction. *J. Am. Chem. Soc.* **1997**, *119*, 9871–9882.
21. Diederich, F.; Thilgen, C. Covalent Fullerene Chemistry. *Science* **1996**, *271*, 317–323.
22. Choi, C. H.; Kertesz, M. New Interpretation of the Valence Tautomerism of 1,6-Methano[10]annulenes and Its Application to Fullerene Derivatives. *J. Phys .Chem. A* **1998**, *102*, 3428–3437.
23. Bettinger, H. F. Addition of Carbenes to the Sidewalls of Single-Walled Carbon Nanotubes. *Chem.—Eur. J.* **2006**, *12*, 4372–4379.
24. More details for the bent graphene model can be seen in Supporting Information.
25. It should be noted here that, for this particular substituent, the open and closed configurations are very close in energy for (5,5) bent graphene, in real (5,5) CNT $C_5O_2H_4$-keto actually gives an open configuration.
26. Lee, Y.-S. Ph.D. Thesis, Massachusetts Institute of Technology: Cambridge, MA, 2006.
27. Coleman, K. S.; Bailey, S. R.; Fogden, S.; Green, M. L. H. Functionalization of Single-Walled Carbon Nanotubes *via* the Bingel Reaction. *J. Am. Chem. Soc.* **2003**, *125*, 8722.
28. Doltsinis, N. L.; Marx, D. Nonadiabatic Car−Parrinello Molecular Dynamics. *Phys. Rev. Lett.* **2002**, *88*, 166402.
29. Handta, J.; Kunertb, T.; Schmidt, R. Fragmentation and cis−trans Isomerization of Diimide in fs Laser-Pulses. *Chem. Phys. Lett.* **2006**, *428*, 220–226.
30. Ben-Nun, M.; Martiez, T. J. Photodynamics of Ethylene: *Ab Initio* Studies of Conical Intersections. *Chem. Phys.* **2000**, *259*, 237–248.
31. Perdew, J.; Burke, K.; Ernzerhof, M. Generalized Gradient Approximation Made Simple. *Phys. Rev. Lett.* **1996**, *77*, 3865–3868.
32. Vanderbilt, D. Soft Self-Consistent Pseudopotentials in a Generalized Eigenvalue Formalism. *Phys. Rev. B* **1990**, *41*, 7892–7895.
33. Giannozzi, P.; Baroni, S.; Bonini, N.; Calandra, M.; Car, R.; Cavazzoni, C.; Ceresoli, D.; Chiarotti, G. L.; Cococcioni, M.; Dabo, I.; *et al.* Quantum-Espresso: A Modular and Open-Source Software Project for Quantum Simulations of Materials. *J. Phys.: Condens. Matter* **2009**, *21*, 395502.
34. Henkelman, G.; Jonsson, H. Improved Tangent Estimate in the Nudged Elastic Band Method for Finding Minimum Energy Paths and Saddle Points. *J. Chem. Phys.* **2000**, *113*, 9978.
35. Marzari, N.; Vanderbilt, D.; Vita, A. D.; Payne, M. C. Thermal Contraction and Disordering of the Al(110) Surface. *Phys. Rev. Lett.* **1999**, *82*, 3296–3299.
36. Landauer, R. Electrical Resistance of Disordered One-Dimensional Lattices. *Philos. Mag.* **1970**, *21*, 863–867.
37. Mostofi, A. A.; Yates, J. R.; Lee, Y.-S.; Souza, I.; Vanderbilt, D.; Marzari, N. Wannier90: A Tool for Obtaining Maximally-Localised Wannier Functions. *Comput. Phys. Commun.* **2008**, *178*, 685.